



Synthesis and characterization of $\text{Ba}_{1-x}\text{Nd}_x\text{F}_{2+x}$ ($0.00 \leq x \leq 1.00$)

V. Grover, S.N. Achary, S.J. Patwe, A.K. Tyagi*

Applied Chemistry Division, Bhabha Atomic Research Centre, Mumbai 400 085, India

Received 6 June 2002; received in revised form 10 December 2002; accepted 27 January 2003

Abstract

A series of mixed fluorides with general composition $\text{Ba}_{1-x}\text{Nd}_x\text{F}_{2+x}$ ($0.00 \leq x \leq 1.00$) was prepared by vacuum heat treatment of the mixture of starting fluorides, and analyzed by powder XRD. From the XRD analysis, the low temperature phase equilibria in BaF_2 – NdF_3 system is elucidated. The initial compositions in this series, that is, up to the nominal composition $\text{Ba}_{0.65}\text{Nd}_{0.35}\text{F}_{2.35}$ ($x \leq 0.35$) exist as cubic fluorite-type solid solution. Beyond the solid solution limit, that is, $x > 0.35$, a rhombohedral fluorite related ordered phase is observed. Further, NdF_3 -rich compositions ($x \geq 0.50$) exist as a mixture of rhombohedral ordered phase and NdF_3 (tysonite)-type phase. About 10 mol% of BaF_2 could be retained in the NdF_3 lattice, forming a tysonite-type solid solution, under the short annealed and slow cooled conditions.

© 2003 Elsevier Science Ltd. All rights reserved.

Keywords: A. Fluorides; C. X-ray diffraction; D. Phase equilibria

1. Introduction

Mixed fluorides of alkaline-earths (MF_2) and rare-earths ($\text{M}'\text{F}_3$) are an important class of inorganic materials owing to their promising applications in the stimulated emission and up conversion processes [1], and various electrical applications [2] such as ion selective electrodes. Thus, the quest for new stable phases and delineation of homogeneity width of solid solutions are enough motivation to study the phase relation in these systems under different experimental conditions. The phase relation in MF_2 – $\text{M}'\text{F}_3$ systems usually consists of a fluorite-type solid solution and tysonite phase or tysonite-type solid solution. In between these two, several ordered lattices either related to the fluorite or tysonite structures were also found to exist. Greis and Haschke [3] had studied the phase relation in MF_2 – $\text{M}'\text{F}_3$ systems under the high temperature and long anneal conditions to reveal the high temperature phase equilibria. Sobolev and coworkers [4–6] have reported similar high temperature phase relations, based on the phase analysis of the samples quenched from high temperature. Several low temperature phase

* Corresponding author. Fax: +91-22-2550-5151/2551-9613.

E-mail address: aktyagi@magnum.barc.ernet.in (A.K. Tyagi).

relations in $\text{MF}_2\text{--M}'\text{F}_3$ ($\text{M}' = \text{Y}^{3+}$, Er^{3+} , and Eu^{3+}) systems based on the phase analysis of the samples obtained after short annealing and slow cooling to room temperature have also been reported [7–10].

The rare-earth trifluorides crystallize in two different modifications, namely hexagonal (tysonite, LaF_3) and orthorhombic ($\beta\text{-YF}_3$) structure. Earlier, several low temperature phase equilibria were reported with orthorhombic-type rare-earth fluorides ($\text{M}^{3+} = \text{Y}^{3+}$, Er^{3+} or Eu^{3+}) [7–10]. In order to study the effect of tysonite-type rare-earth fluorides on the $\text{MF}_2\text{--M}'\text{F}_3$ phase relation, investigations on $\text{BaF}_2\text{--NdF}_3$ system have been under taken.

The phase diagram of $\text{BaF}_2\text{--NdF}_3$ system above 800°C , has been reported by Tkachenko et al. [11] and Sobolev and Tkachenko [4]. It was observed in these studies that $\text{BaF}_2\text{--NdF}_3$ system has only two distinct phases, namely, a fluorite-type solid solution towards the BaF_2 -rich end and a tysonite-type solid solution towards the NdF_3 -rich end. However, for YF_3 -type rare-earth fluorides a rhombohedral phase for the composition containing about 45 mol% of $\text{M}'\text{F}_3$ and a monoclinic phase with the composition $\text{BaM}'_2\text{F}_8$ were also reported. Kieser and Greis [12] had shown that a rhombohedral phase exists with the tysonite-type fluorides also, namely CeF_3 and NdF_3 . Although the studies of Sobolev and Tkachenko [4] were based on the high temperature quenched samples, still the rhombohedral phase was not detected. Sobolev and Tkachenko [4] have reported the solid solution limit of NdF_3 in BaF_2 lattice and BaF_2 in NdF_3 lattice to be approximately 50 and 19 mol%, respectively. Since the phase relation data available in $\text{BaF}_2\text{--NdF}_3$ system were collected using the high temperature quenched samples, it cannot be extended to establish low temperature phase equilibria. Hence, the low temperature phase equilibria in $\text{BaF}_2\text{--NdF}_3$ system has been studied in the present investigations. The details of the phase analysis are discussed, and compared to the earlier reported high temperature phase equilibria.

2. Experimental

NdF_3 was prepared by fluoridating Nd_2O_3 with NH_4HF_2 . The fluoridation was carried out at 450°C with repeated addition of excess of NH_4HF_2 . The product obtained by this process was further dried at 450°C under a flowing argon atmosphere. BaF_2 was prepared as the procedure followed in earlier studies [7–10]. The mixed fluoride compositions were prepared by heating the appropriate mixture at 900°C for 8 h under a static vacuum, followed by cooling to room temperature at the rate of $2^\circ\text{C}/\text{min}$. The various nominal compositions obtained were characterized by powder XRD using a monochromatic $\text{Cu K}\alpha$ radiation on a Philips X-ray diffractometer, Model PW 1729.

3. Results and discussions

NdF_3 and BaF_2 were characterized by comparing their XRD patterns to the reported ones (JC-PDS cards). The powder XRD patterns of various nominal compositions $\text{Ba}_{1-x}\text{Nd}_x\text{F}_{2+x}$ ($0.00 \leq x \leq 1.00$) were analyzed either by comparing the successive compositions or to any reported iso-structural phase. Some typical XRD patterns are shown in Fig. 1. The details of the phase analysis are given in Table 1, and explained as the following.

The end members BaF_2 and NdF_3 subjected to the same experimental conditions are also included in Table 1 for the comparison. The XRD patterns of nominal compositions following BaF_2 ($x = 0.00$) namely, $\text{Ba}_{0.95}\text{Nd}_{0.05}\text{F}_{2.05}$ ($x = 0.05$) and so on up to $\text{Ba}_{0.65}\text{Nd}_{0.35}\text{F}_{2.35}$ ($x = 0.35$), appear similar to that

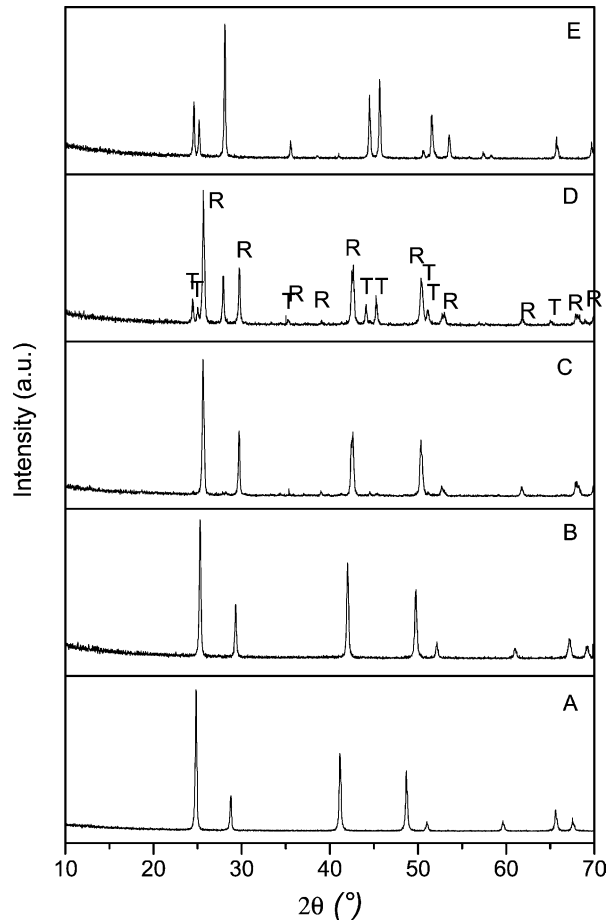


Fig. 1. Powder XRD patterns of some typical compositions. (A) $\text{Ba}_{1.00}\text{Nd}_{0.00}\text{F}_{2.00}$, (B) $\text{Ba}_{0.70}\text{Nd}_{0.30}\text{F}_{2.30}$, (C) $\text{Ba}_{0.55}\text{Nd}_{0.45}\text{F}_{2.45}$, (D) $\text{Ba}_{0.40}\text{Nd}_{0.60}\text{F}_{2.60}$ (T: tysonite; R: rhombohedral), and (E) $\text{Ba}_{0.00}\text{Nd}_{1.00}\text{F}_{3.00}$.

of pure BaF_2 . This indicates that the BaF_2 lattice is retained in these compositions and they exist as solid solutions. This is the typical observation in all MF_2 -rich compositions in the MF_2 - $\text{M}'\text{F}_3$ systems, irrespective of the experimental conditions.

The typical fluorite-type reflections were observed up to the nominal composition $\text{Ba}_{0.65}\text{Nd}_{0.35}\text{F}_{2.35}$. A comparison of these XRD patterns implies that the position of the fluorite reflections shift gradually towards the higher angle side. This indicates that the BaF_2 lattice contracts with the addition of NdF_3 (Table 1). A plot of the unit cell parameters with the mol% of the NdF_3 in the lattice is shown in Fig. 2, which implies its linear dependence on the mol% of NdF_3 . The typical linear fit of the unit cell parameter to the mol% of NdF_3 in BaF_2 lattice is given as

$$a (\text{\AA}) = 6.196(2) - 0.004 \times [X]$$

where X = mol% of NdF_3 in $\text{Ba}_{1-x}\text{Nd}_x\text{F}_{2+x}$ solid solutions.

The nature of the fluorite-type solid solution formed in the BaF_2 - NdF_3 system is expected to be quite similar to that observed in other systems like BaF_2 - YF_3 [8] and BaF_2 - ErF_3 [9]. The structural details of

Table 1
Ba_{1-x}Nd_xF_{2+x} compositions and their phase analyses

S. no.	Compositions	mol% of NdF ₃	Phases identified	<i>a</i> (Å)	<i>b</i> (Å)	<i>c</i> (Å)	<i>V</i> (Å) ³
1	Ba _{1.00} Nd _{0.00} F _{2.00}	0	C	6.200(1)	6.200(1)	6.200(1)	238.29(4)
2	Ba _{0.95} Nd _{0.05} F _{2.05}	5	C	6.171(0)	6.171(0)	6.171(0)	235.04(1)
3	Ba _{0.90} Nd _{0.10} F _{2.10}	10	C	6.151(1)	6.151(1)	6.151(1)	232.75(7)
4	Ba _{0.85} Nd _{0.15} F _{2.15}	15	C	6.128(1)	6.128(1)	6.128(1)	230.11(3)
5	Ba _{0.80} Nd _{0.20} F _{2.20}	20	C	6.103(2)	6.103(2)	6.103(2)	227.28(10)
6	Ba _{0.75} Nd _{0.25} F _{2.25}	25	C	6.077(1)	6.077(1)	6.077(1)	224.47(5)
7	Ba _{0.70} Nd _{0.30} F _{2.30}	30	C	6.075(3)	6.075(3)	6.075(3)	224.20(17)
8	Ba _{0.65} Nd _{0.35} F _{2.35}	35	C	6.040(1)	6.040(1)	6.040(1)	220.33(7)
9	Ba _{0.60} Nd _{0.40} F _{2.40}	40	R	4.266(1)	4.266(1)	10.415(10)	164.1(2)
10	Ba _{0.55} Nd _{0.45} F _{2.45}	45	R	4.257(1)	4.257(1)	10.361(3)	162.6(1)
11	Ba _{0.50} Nd _{0.50} F _{2.50}	50	R H ^a	4.251(1)	4.251(1)	10.347(2)	162.0(0)
12	Ba _{0.45} Nd _{0.55} F _{2.55}	55	R H	4.228(0)	4.228(0)	10.366(2)	160.4(1)
13	Ba _{0.40} Nd _{0.60} F _{2.60}	60	R H	4.241(5) 7.110(10)	4.241(5) 7.110(10)	10.41(2) 7.26(1)	162.1(4) 317.9(8)
14	Ba _{0.35} Nd _{0.65} F _{2.65}	65	R H	4.239(5) 7.112(4)	4.239(5) 7.112(4)	10.35(2) 7.263(4)	161.1(4) 318.1(3)
15	Ba _{0.30} Nd _{0.70} F _{2.70}	70	R H	4.252(5) 7.113(2)	4.252(5) 7.113(2)	10.39(1) 7.275(2)	162.6(3) 318.7(1)
16	Ba _{0.25} Nd _{0.75} F _{2.75}	75	R H	4.242(2) 7.117(1)	4.242(2) 7.117(1)	10.339(7) 7.276(1)	161.2(2) 319.1(1)
17	Ba _{0.20} Nd _{0.80} F _{2.80}	80	R H	4.245(7) 7.106(2)	4.245(7) 7.106(2)	10.41(2) 7.270(2)	162.4(5) 317.9(1)
18	Ba _{0.15} Nd _{0.85} F _{2.85}	85	R ^a H	7.119(2)	7.119(2)	7.283(2)	319.7(2)
19	Ba _{0.10} Nd _{0.90} F _{2.90}	90	R ^a H	7.106(4)	7.106(4)	7.256(4)	317.3(3)
20	Ba _{0.05} Nd _{0.95} F _{2.95}	95	H	7.068(1)	7.068(1)	7.231(2)	312.8(1)
21	Ba _{0.00} Nd _{1.00} F _{3.00}	100	H	7.039(2)	7.039(2)	7.206(3)	309.1(2)

C: cubic fluorite-type phase; R: rhombohedral ordered phase; H: NdF₃ phase.

^a Not refined due to insignificant intensity or overlapping reflections.

such solid solutions have been explained in the study of BaF₂–EuF₃ system [10]. Based on the density variation [13] and neutron diffraction studies [14], the fluorite-type solid solutions have been shown to contain an anion-excess instead of a cation-deficiency. The Ba²⁺ and Nd³⁺ ions are statistically distributed in the 4*a* site of the space group Fm3*m*. The anions occupy the interstices of the type 32*f* or 48*i* in addition to the normal 8*c* site of the fluorite structure. As the Nd³⁺ ion has smaller ionic radius compared to that of Ba²⁺, the average ionic radius of this site decreases, which causes the lattice contraction. In addition, the extra-anions are incorporated in to the unit cell for charge compensation, which causes the inter-anionic repulsion and in turn the dilation of the unit cell. Thus, these two effects

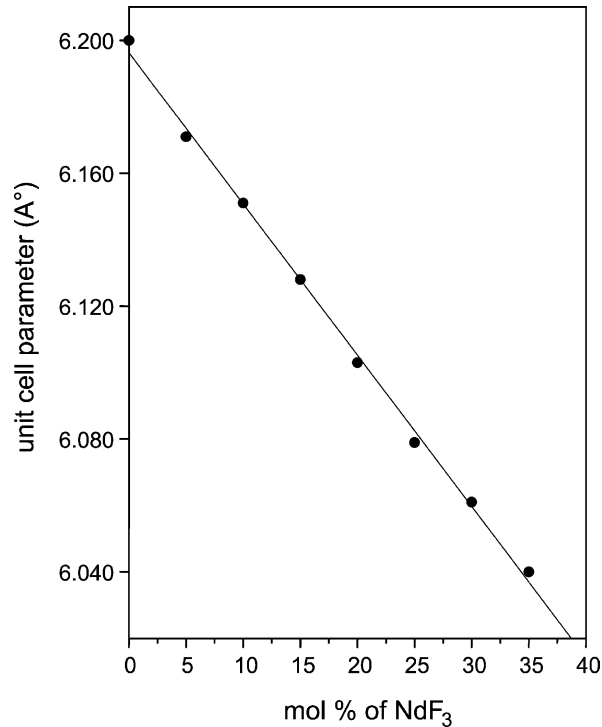


Fig. 2. Variation of the unit cell parameter with mol% of NdF₃ within the fluorite-type solid solutions.

in combination govern slope of the straight line representing the unit cell parameter versus composition. Since the ionic radii of rare-earth ions are smaller compared to that of Ba²⁺, the unit cell parameters always decrease in BaF₂–M'F₃ systems, as observed earlier also [8–10].

Under the present experimental conditions, the solid solution limit of NdF₃ in BaF₂ is found to be about 35 mol%. Tkachenko et al. [11] and Sobolev and Tkachenko [4] have reported that about 50 mol% of NdF₃ can be retained in the fluorite lattice. Since they have analyzed the high temperature quenched samples, the higher homogeneity width is expected. However, Kieser and Greis [12] have reported the Ba₄M₃F₁₇ (i.e. Ba_{0.57}Nd_{0.43}F_{2.43})-type phase also in high temperature long annealed samples. Since they did not report the detailed phase equilibria, it is assumed that the solid solution limit, under their experimental conditions, must be less than 43 mol% of NdF₃. Under the present experimental conditions, the BaF₂–YF₃ [8] and BaF₂–ErF₃ [9] were shown to have a fluorite-type solid solution limit of about 25 mol%, while that in BaF₂–EuF₃ system [10] is about 30 mol%. The corresponding value found in BaF₂–NdF₃ system shows that the solid solution limit increases as the cationic size difference decreases. A similar conclusion was also reported in the CaF₂–YF₃ system [15].

The XRD pattern of the nominal composition Ba_{0.60}Nd_{0.40}F_{2.40} ($x = 0.40$) shows the presence of the typical fluorite reflections, however, the reflections at the $2\theta \approx 25, 42,$ and 50° corresponding to the (1 1 1), (2 2 0) and (3 1 1) planes were found to split, which indicates a distortion in the fluorite lattice. It may be noted that the other fluorite reflections that remain are not split, which would have been a case if this composition was a mixture of two fluorite-type phases. Thus, it was inferred that Ba_{0.60}Nd_{0.40}F_{2.40} is a single phasic composition. In addition, the XRD pattern of this phase shows the

presence of some weak reflections at $2\theta \approx 39, 41, 44,$ and 45° . This indicates that an ordered structure, closely related to the fluorite lattice, starts forming at this composition. The weak reflections observed become prominent at the nominal composition $\text{Ba}_{0.55}\text{Nd}_{0.45}\text{F}_{2.45}$ ($x = 0.45$). Beyond this composition, the other nominal compositions, that is, for $x \geq 0.50$, show the presence of the unreacted, that is, NdF_3 , which indicates that this phase exists at the compositions containing 40–45 mol% of NdF_3 in BaF_2 (i.e. with $0.40 \leq x \leq 0.45$). Such ordered phases were reported in earlier studies also, namely in the $\text{BaF}_2\text{--M}'\text{F}_3$, ($\text{M}' = \text{Y}^{3+}, \text{Er}^{3+},$ and Eu^{3+}) [8–10] systems. The intense reflections observed for the nominal composition $\text{Ba}_{0.55}\text{Nd}_{0.45}\text{F}_{2.45}$ ($x = 0.45$), excluding the weak reflections, could be indexed on a rhombohedral lattice with unit cell parameters, $a = 4.239(1) \text{ \AA}$ and $\alpha = 60.29(2)^\circ$. The corresponding hexagonal unit cell parameters are: $a = 4.257(1)$ and $c = 10.361(3) \text{ \AA}$. However, all the observed reflections including the weak reflections could be indexed on a larger rhombohedral unit cell, which is closely related to the smaller one. The typical unit cell parameters for this phase are: $a = 11.268(2)$, $c = 20.715(5) \text{ \AA}$, and $V = 2277.8(8) \text{ \AA}^3$ (i.e. $a = 9.487(2) \text{ \AA}$, $\alpha = 72.86(2)^\circ$, and $V = 759.2(3) \text{ \AA}^3$ in rhombohedral settings). A comparison of the unit cell to the earlier reported rhombohedral unit cells [8–10] shows that they are remarkably similar to each other, and also to the $\text{Rh}\alpha$ phase reported by Greis and Haschke [3]. The list of the observed and calculated reflections for the nominal compositions $\text{Ba}_{0.60}\text{Nd}_{0.40}\text{F}_{2.40}$ and $\text{Ba}_{0.55}\text{Nd}_{0.45}\text{F}_{2.45}$ ($x = 0.40$ and 0.45) are given in the Tables 2 and 3, respectively.

Table 2

Fit for the nominal composition $\text{Ba}_{0.60}\text{Nd}_{0.40}\text{F}_{2.40}$

S. no.	$d_{(\text{obs})}$ (\AA)	I/I_0 (%)	Hexagonal settings ^a		Rhombohedral settings ^b	
			hkl	$d_{(\text{cal})}$ (\AA)	hkl	$d_{(\text{cal})}$ (\AA)
1	3.487	100	2 1 2	3.481	2 1 –1	3.484
2	3.474	72	0 0 6	3.473	2 2 2	3.464
3	3.008	33	2 1 4	3.013	3 1 0	3.012
4	2.312	2	2 1 7	2.318	4 2 1	2.316
5	2.187	2	3 2 2	2.191	3 –2 1	2.190
6	2.135	42	4 1 0	2.132	3 –2 –1	2.132
7	2.128	43	2 1 8	2.129	4 3 1	2.127
8	2.034	1	4 1 3	2.038	4 –1 0	2.038
					3 2 –2	2.040
9	1.817	29	4 1 6	1.817	4 3 –1	1.818
			3 3 3	1.815	5 1 0	1.817
10	1.795	4	3 2 7	1.791	5 2 0	1.791
11	1.741	7	4 2 4	1.740	4 2 –2	1.742
12	1.733	5	5 1 2	1.730	4 4 4	1.732
					3 –3 2	1.730
13	1.507	4	4 2 8	1.506	6 2 0	1.506
14	1.483	1	6 1 1	1.486	4 –3 –2	1.486
15	1.383	8	4 4 3	1.380	5 –3 1	1.381

Unit cell parameters.

^a $a = 11.282(6) \text{ \AA}$, $c = 20.84(3) \text{ \AA}$, and $V = 2297(4) \text{ \AA}^3$.^b $a = 9.523(7) \text{ \AA}$, $\alpha = 72.62(7)^\circ$, and $V = 765.4(8) \text{ \AA}^3$.

Table 3
Fit for the nominal composition $\text{Ba}_{0.55}\text{Nd}_{0.45}\text{F}_{2.45}$

S. no.	$d_{(\text{obs})}$ (Å)	I/I_0 (%)	Hexagonal settings ^a		Rhombohedral settings ^b	
			hkl	$d_{(\text{cal})}$ (Å)	hkl	$d_{(\text{cal})}$ (Å)
1	3.476	100	2 1 2	3.475	2 1 -1	3.475
2	3.455	38	0 0 6	3.453	2 2 2	3.452
3	3.006	49	2 1 4	3.004	3 1 0	3.004
4	2.308	3	2 1 7	2.308	4 2 1	2.308
5	2.187	2	3 2 2	2.188	3 -2 1	2.188
6	2.129	45	4 1 0	2.129	3 -2 -1	2.129
7	2.119	43	2 1 8	2.119	4 3 1	2.119
8	2.053	1	3 2 4	2.055	4 1 -1	2.055
9	2.032	3	4 1 3	2.035	4 -1 0	2.035
					3 2 -2	2.035
10	2.000	2	3 1 7	1.997	4 3 0	1.997
11	1.813	41	4 1 6	1.812	4 3 -1	1.812
			3 3 3	1.812	5 1 0	1.812
12	1.806	21	2 1 10	1.806	5 3 2	1.806
13	1.786	3	3 2 7	1.785	5 2 0	1.785
14	1.737	9	4 2 4	1.737	4 2 -2	1.737
15	1.727	3	5 1 2	1.728	3 -3 2	1.728
			0 0 12	1.726	4 4 4	1.726
16	1.502	7	4 2 8	1.502	6 2 0	1.502
17	1.485	2	6 1 1	1.484	4 -3 -2	1.484
18	1.381	12	4 4 3	1.380	5 -3 1	1.380
19	1.373	7	2 1 14	1.373	6 5 3	1.373
			3 1 13	1.373	6 5 2	1.373

Unit cell parameters.

^a $a = 11.268(2)$ Å, $c = 20.715(5)$ Å, and $V = 2277.8(8)$ Å³.

^b $a = 9.487(2)$ Å, $\alpha = 72.86(2)^\circ$, and $V = 759.2(3)$ Å³.

The above rhombohedral phase is found to be present in all the nominal compositions following $\text{Ba}_{0.55}\text{Nd}_{0.45}\text{F}_{2.45}$, that is, $x \geq 0.45$. The intensity of the reflections attributable to this rhombohedral phase decreases on going towards NdF_3 end. The rhombohedral phases observed in various nominal compositions are included in Table 1, along with the basis unit cell parameters. A comparison of the unit cell volume shows that it decreases significantly from the composition $\text{Ba}_{0.60}\text{Nd}_{0.40}\text{F}_{2.40}$ to $\text{Ba}_{0.55}\text{Nd}_{0.45}\text{F}_{2.45}$, and then onwards it remains almost unchanged. It indicates that this phase can sustain slight deviation from the ideal-stoichiometry and has a narrow phase width, which is also in agreement with a few earlier reports [8–10]. The corresponding stoichiometric composition of this phase is expected to be $\text{Ba}_{0.57}\text{Nd}_{0.43}\text{F}_{2.43}$ (i.e. $\text{Ba}_4\text{Nd}_3\text{F}_{17}$), which was prepared under similar experimental conditions. The unit cell parameters of the basis cell of this particular phase are: $a = 4.265(1)$, $c = 10.394(7)$ Å, and $V = 163.8(1)$ Å³, the corresponding rhombohedral unit cell parameters are $a = 4.250(2)$ Å, $\alpha = 60.24(4)^\circ$, and $V = 54.58(4)$ Å³. The typical unit cell parameters of the corresponding rhombohedral super-structure are $a = 11.281(2)$, $c = 20.783(7)$ Å, and

$V = 2290.5(9) \text{ \AA}^3$. The structure of this phase has been elucidated by Rietveld refinement of the powder X-ray data and explained elsewhere [16]. The observed and calculated intensities for this phase were also explained therein. Earlier Kieser and Greis [12] had reported that the rhombohedral $\text{Ba}_4\text{M}'_3\text{F}_{17}$ ($\text{Ba}_{0.57}\text{M}'_{0.43}\text{F}_{2.43}$) phase exists with CeF_3 , PrF_3 , and NdF_3 (all tysonite-type) in addition to all the rare-earth fluorides of YF_3 structure. Later these phases were also characterized [16] by electron diffraction. In these studies, the ordering was reported after long annealing at elevated temperature, namely 38 days for tysonite-type rare-earth fluorides and 29 days for YF_3 -type rare-earth fluorides. In the present investigations, it was remarkably observed that just a very short annealing time is sufficient for the formation of ordered phase, even for tysonite-type rare-earth fluorides. Thus, it can be concluded that the predominant driving force for ordering is the difference in the ionic radii of the cations (ionic radii of Nd^{3+} , Eu^{3+} , and Y^{3+} are 1.11, 1.07, and 1.02 \AA , respectively, compared to Ba^{2+} with ionic radius as 1.42 \AA , all in eight-fold coordination Table 4).

Table 4
Fit for the nominal composition $\text{Ba}_4\text{Nd}_3\text{F}_{17}$

$d_{(\text{obs})}$ (\AA)	I/I_0 (%)	Hexagonal lattice parameters		Rhombohedral lattice parameters		Hexagonal basis unit cell parameters		Rhombohedral basis unit cell parameters	
		hkl	$d_{(\text{cal})}$	hkl	$d_{(\text{cal})}$	hkl	$d_{(\text{cal})}$	hkl	$d_{(\text{cal})}$
3.484	100	2 1 2	3.479	2 1 -1	3.479	1 0 1	3.481	1 0 0	3.481
3.010	43	2 1 4	3.010	3 1 0	3.010	1 0 2	3.011	1 1 0	3.011
2.313	3	2 1 7	2.314	4 2 1	2.314				
2.135	43	1 1 9	2.137	4 3 2	2.137	1 1 0	2.133	1 -1 0	2.133
2.125	37	2 1 8	2.125	4 3 1	2.125	1 0 4	2.125	2 1 1	2.125
2.037	5	4 1 3	2.038	3 2 -2	2.037				
				4 -1 0	2.037				
2.002	1	3 1 7	2.001	4 3 0	2.001				
1.838	2	4 2 1	1.839	3 -3 1	1.839	1 1 3	1.816	2 1 0	1.816
1.816	40	4 1 6	1.816	4 3 -1	1.815	1 0 5	1.812	2 2 1	1.811
				5 1 0	1.816				
1.813	36	3 3 3	1.815	4 -2 1	1.814				
1.786	2	2 2 9	1.787	5 3 1	1.787				
1.739	10	4 2 4	1.740	4 2 -2	1.740	2 0 2	1.740	2 0 0	1.740
1.504	8	4 2 8	1.505	6 2 0	1.505	2 0 4	1.505	2 2 0	1.505
1.384	11	5 3 2	1.383	4 -3 -3	1.383	2 1 1	1.384	2 -1 0	1.384
		7 0 2	1.383	5 -3 0	1.383				
1.378	8	2 1 14	1.377	6 5 3	1.377				
1.347	8	5 3 4	1.348	6 -1 -1	1.348				
		7 0 4	1.348	5 -3 2	1.348				
1.331	1	6 0 9	1.331	5 5 -1	1.331				

Hexagonal lattice parameters: $a = 11.281(2) \text{ \AA}$, $c = 20.783(7) \text{ \AA}$, and $V = 2290.5(9) \text{ \AA}^3$. Rhombohedral lattice parameters: $a = 9.508(2) \text{ \AA}$, $\alpha = 72.76(2)^\circ$, and $V = 763.4(2) \text{ \AA}^3$. Hexagonal basis unit cell parameters: $a = 4.265(1) \text{ \AA}$, $c = 10.394(7) \text{ \AA}$, and $V = 163.8(1) \text{ \AA}^3$. S: Rhombohedral basis unit cell parameters: $a = 4.250(2) \text{ \AA}$, $\alpha = 60.24(4)^\circ$, and $V = 54.58(4) \text{ \AA}^3$. (The presence and absence of certain, namely (0 0 6) reflections in the observed reflection list of the Tables 2–4 may be attributed to the overlapping of the closely spaced peaks.)

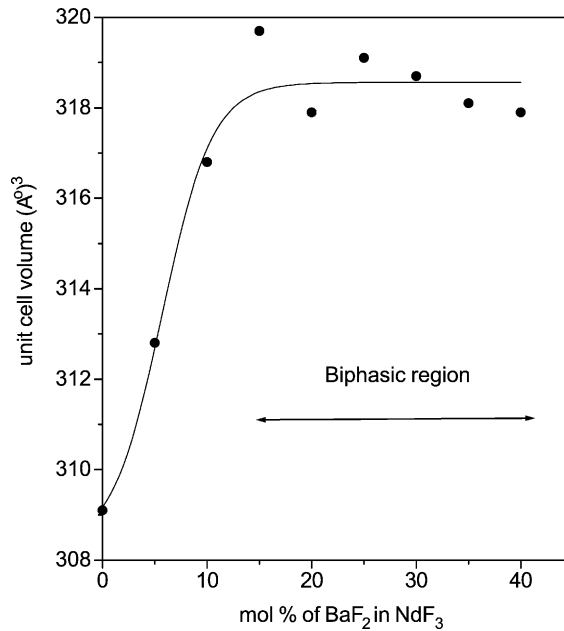


Fig. 3. Variation of the unit cell volume with mol% of BaF₂ within the tysonite-type solid solutions.

The XRD patterns of the nominal compositions following the composition Ba_{0.55}Nd_{0.45}F_{2.45}, that is, with $x \geq 0.45$, namely, Ba_{0.50}Nd_{0.50}F_{2.50}, Ba_{0.45}Nd_{0.55}F_{2.55}, Ba_{0.40}Nd_{0.60}F_{2.60} etc. indicate the presence of a NdF₃-type (tysonite) phase in addition to a rhombohedral phase. This indicates that there are no other ordered mixed fluoride compounds in BaF₂–NdF₃ system except the above-mentioned rhombohedral compound. The selected reflections attributable to the NdF₃-type phase could be indexed on a hexagonal lattice. The unit cell parameters of this phase, identified in various nominal compositions, are included in Table 1. A careful analysis of the XRD patterns of nominal composition Ba_{0.10}Nd_{0.90}F_{2.90} ($x = 0.90$) shows the presence of a very small amount of the earlier described rhombohedral phase. The next nominal composition at $x = 0.95$ does not show even trace of this phase, which suggests the formation of tysonite-type solid solution. A comparison of the unit cell parameters of the later phases shows an increase of unit cell volume with the BaF₂ content in the NdF₃ lattice consistent with tysonite-type solid solution formation. This trend in the unit cell volume of NdF₃ (tysonite)-type phases can be attributed to higher ionic radii of the Ba²⁺ ion compared to Nd³⁺.

The variation of unit cell volume of the tysonite-type phases with mol% of BaF₂ is given in Fig. 3. A comparison of unit cell volume of the tysonite-type phases shows an increase up to 15 mol% of BaF₂. The unit cell volume of the tysonite-type phase remains almost similar on further increase of the BaF₂ content. An extrapolation of the unit cell volumes from both end-compositions with tysonite lattice indicates the solid solution limit of BaF₂ in the NdF₃ lattice to be within 10–15 mol%. It has been mentioned in the earlier section that the XRD pattern of Ba_{0.10}Nd_{0.90}F_{2.90} has a reflection at $2\theta \approx 25.64^\circ$ attributable to the rhombohedral phase. The intensity of this reflection increases significantly as the composition changed to Ba_{0.15}Nd_{0.85}F_{2.85}. Although the comparison of unit cell volumes suggests the solid solution limit close to 12 mol% of BaF₂, the presence of rhombohedral phase reflection in XRD pattern of Ba_{0.10}Nd_{0.90}F_{2.90} indicates the solubility limit should be closer to

10 mol%. In a parallel study, $\text{CaF}_2\text{--NdF}_3$ and $\text{SrF}_2\text{--NdF}_3$ systems were also investigated under the similar conditions [17]. In the $\text{SrF}_2\text{--NdF}_3$ system it was found that the unit cell volume of the tysonite lattice increases from $\text{Sr}_{0.00}\text{Nd}_{1.00}\text{F}_{3.00}$ ($V = 309.1 \text{ \AA}^3$) to $\text{Sr}_{0.10}\text{Nd}_{0.90}\text{F}_{2.90}$ ($V = 311.1 \text{ \AA}^3$) and then onwards there was no significant variation. In the $\text{CaF}_2\text{--NdF}_3$ system it was observed that the unit cell volume of NdF_3 lattice decreases up to $\text{Ca}_{0.20}\text{Nd}_{0.80}\text{F}_{2.80}$ (304.9 \AA^3), which was identified as a mixture of tysonite- and fluorite-type phase). The compositions beyond $\text{Ca}_{0.20}\text{Nd}_{0.80}\text{F}_{2.80}$, towards the CaF_2 end, remain as biphasic without change in their unit cell volumes. From this it was concluded that the typical solid solution limits of CaF_2 and SrF_2 in NdF_3 are close to 15 and 10 mol%, respectively [17]. A comparison of these three systems further suggests that the solid solution limit of BaF_2 in NdF_3 should be close to 10 mol%.

Although the ionic radius of Nd^{3+} is much smaller than that of Ba^{2+} , the solid solubility of BaF_2 in NdF_3 is observed. Earlier reports of Tkachenko et al. [11] and Sobolev and Tkachenko [4] have also indicated the formation of solid solution in the tysonite-type lattice. In the $\text{BaF}_2\text{--NdF}_3$ system (above $800 \text{ }^\circ\text{C}$), about 19 mol% BaF_2 was reported to form solid solution with tysonite-type lattice [4,18]. The low solid solubility limit, as observed in the present study, can be attributed to slow cooling condition. The tysonite-type structure can be stabilized in the heavier rare-earth fluorides either by creation of vacancies in the anionic sub-lattice [18,19] or by the increase of the average cation radii with the substitution of larger cations [20]. In the orthorhombic rare-earth fluorides, this structure is often observed as the bertholide type.

4. Conclusions

A systematic XRD study on the complete range of nominal compositions $\text{Ba}_{1-x}\text{Nd}_x\text{F}_{2+x}$ ($0.00 \leq x \leq 1.00$) prepared under short annealed and slow cooled conditions, revealed a low temperature phase equilibria in $\text{BaF}_2\text{--NdF}_3$ system. The $\text{BaF}_2\text{--NdF}_3$ system consists of fluorite-type solid solution towards the BaF_2 -rich, that is, for $x \leq 0.35$ end and tysonite-type solid solution at the NdF_3 rich end, that is, for $x \geq 0.90$. In addition, a fluorite-related rhombohedral phase is observed for $0.40 \leq x \leq 0.45$. The unit cell volume of both the fluorite-type solid solution and tysonite-type solid solution decrease with increase in the NdF_3 mol%.

Acknowledgements

We thank Dr. N. M. Gupta, Head, Applied Chemistry Division for his interest in this work.

References

- [1] A.A. Kaminskii, Phys. Stat. Sol. (a) 148 (1995) 9.
- [2] M.S. Frant, J.W. Ross Jr., Science 154 (1966) 1553.
- [3] O. Greis, J.M. Haschke, in: K.A. Gschneidner, L. Eyring (Eds.), Handbook on the Physics and Chemistry of Rare Earths, vol. 45, North-Holland, Amsterdam, 1982, p. 387.
- [4] B.P. Sobolev, N.L. Tkachenko, J. Less Comm. Metals 85 (1982) 155.
- [5] P.P. Fedorov, B.P. Sobolev, J. Less Comm. Metals 63 (1979) 31.

- [6] B.P. Sobolev, K.B. Seiranian, L.S. Garashina, P.P. Fedorov, J. Solid State Chem. 28 (1979) 51.
- [7] S.J. Patwe, S.N. Achary, A.K. Tyagi, Mater. Res. Bull. 36 (2001) 597.
- [8] S.N. Achary, S. Mahapatra, S.J. Patwe, A.K. Tyagi, Mater. Res. Bull. 34 (1999) 1535.
- [9] S.J. Patwe, S.N. Achary, A.K. Tyagi, Mater. Res. Bull. 37 (2002) 2243.
- [10] S.N. Achary, S.J. Patwe, A.K. Tyagi, Mater. Res. Bull. 37 (2002) 2227.
- [11] N.L. Tkachenko, L.S. Garashina, O.E. Izotova, V.B. Aleksandrov, B.P. Sobolev, J. Solid State Chem. 8 (1973) 213.
- [12] V.M. Kieser, O. Greis, Z. Anorg. Allg. Chem. 469 (1980) 164.
- [13] J.M. Short, R. Roy, J. Phys. Chem. 67 (1967) 1860.
- [14] A.K. Cheetham, B.E.F. Fender, M.J. Cooper, J. Phys. C: Solid State Phys. 4 (1971) 3107.
- [15] S.N. Achary, S.J. Patwe, A.K. Tyagi, Mater. Res. Bull. 34 (1999) 2093.
- [16] O. Greis, M. Kieser, J. Less Comm. Metals 75 (1980) 119.
- [17] V. Grover, S. N. Achary, S. J. Patwe, A. K. Tyagi, Mater. Res. Bull. (Communicated).
- [18] B.P. Sobolev, V.B. Aleksandrov, P.P. Fedorov, K.B. Seiranian, N.L. Tkachenko, Sov. Phys. Crystallogr. 21 (1980) 49.
- [19] B.P. Sobolev, P.P. Fedorov, K.B. Seiranian, N.L. Tkachenko, J. Solid State Chem. 17 (1976) 201.
- [20] O.V. Kudryavtseva, L.S. Garashina, K.K. Rivkina, B. P. Sobolev, Sov. Phys. Crystallogr. 18 (1974) 531.